ELSEVIER

European Journal of Pharmacology 306 (1996) 195–210

ejp

# Molecular modeling of serotonin, ketanserin, ritanserin and their 5-$HT_{2C}$ receptor interactions

Kurt Kristiansen, Svein G. Dahl *

*Department of Pharmacology, Institute of Medical biology, University of Tromsö, 9037 Tromsö, Norway*

Received 7 December 1995; revised 22 February 1996; accepted 27 February 1996

**Abstract**

Molecular modeling techniques were used to build a three-dimensional model of the rat 5-$HT_{2C}$ receptor, which was used to examine receptor interactions for protonated forms of serotonin, ketanserin and ritanserin. Molecular dynamics simulations which were started with the fluoro benzene moiety of ketanserin and ritanserin oriented towards the cytoplasmic side of the receptor model, produced the strongest antagonist–receptor interactions. The fluoro benzene ring(s) of the antagonists interacted strongly with aromatic residues in the receptor model, which predicts slightly different orientations and ligand–receptor interactions of ketanserin and ritanserin at a putative binding site. The model suggests that $Asn^{333}$ (transmembrane helix 6) is involved in a hydrogen-bonding interaction with ketanserin, but not with ritanserin. The model also also suggests that the position corresponding to $Cys^{362}$ (transmembrane helix 7) may be an important determinant for specifying 5-$HT_{2A}$ receptor selectivity in ketanserin binding.

*Keywords:* Molecular modeling; Three-dimensional structure; 5-$HT_{2C}$ receptor; Receptor binding; Subtype selectivity

## 1. Introduction

The current classification of 5-hydroxytryptamine (5-HT) receptor subtypes (Peroutka, 1994; Boess and Martin, 1994) is based on pharmacological and functional characteristics and on similarities in primary structure (Humphrey et al., 1993). With exception of the 5-$HT_3$ receptor subtype, all cloned mammalian 5-HT receptor subtypes belong to the superfamily of G-protein-coupled receptors. Among these are the 5-$HT_{2A}$ (formerly 5-$HT_2$), 5-$HT_{2B}$ (formerly 5-$HT_{2F}$) and 5-$HT_{2C}$ (formerly 5-$HT_{1C}$) receptors. The 5-$HT_{2C}$ receptor is expressed in brain and choroid plexus, while the 5-$HT_{2A}$ receptor is expressed in the brain and in the periphery. The 5-$HT_{2B}$ receptor is expressed in rat and mouse stomach fundus, in most peripheral organs in humans and at low levels in the human brain tissues and blood cells (Schmuck et al., 1994). The rat 5-$HT_{2A}$, 5-$HT_{2B}$ and 5-$HT_{2C}$ receptors have 68–79% amino-acid identity in the transmembrane segments (Nelson, 1993). Agonist activation of 5-$HT_{2A}$, 5-$HT_{2B}$ and 5-$HT_{2C}$ receptors activates phospholipase C, which leads to increased inositolphosphatidyl hydrolysis in the cell (Boess and Martin, 1994).

The antagonist, ketanserin, has been one of the most frequently used radioligands in 5-$HT_{2A}$ receptor binding experiments. Ketanserin has a 26-fold higher affinity to rat 5-$HT_{2A}$ receptors than to rat 5-$HT_{2C}$ receptors (Choudhary et al., 1992), very low affinity to rat 5-$HT_{2B}$ receptors (Boess and Martin, 1994) and high affinity to rat brain $\alpha_1$ adrenergic receptors (Van Wijngaarden et al., 1990). Ketanserin decreases basal 5-$HT_{2C}$ receptor activation (agonist-independent stimulation of phosphatidyl hydrolysis) by binding with higher affinity to the uncoupled form of the receptor, shifting receptor equilibrium away from the precoupled state (Westphal and Sanders-Bush, 1994; Barker et al., 1994). Two other antagonists, MDL 100, 907 ((+)-α-(2,3-dimethoxyphenyl)-1-[2-(4-fluorophenylethyl)]-4-piperidinemethanol) (Dudley et al., 1990) and *N*-(4-phenylbutyl)-4-(4-fluorobenzoyl)piperidine (Herndon et al., 1992), are more selective for the 5-$HT_{2A}$ receptor than is ketanserin. *N*-(4-bromobenzyl)-substituted phenylalkylamine and indolylalkylamine derivatives have been reported to bind to the 5-$HT_{2A}$ receptor as agonists with high affinity ($K_i < 1$ nM) and with > 100-fold selectivity (Glennon et al., 1994). However, no highly selective 5-$HT_{2C}$ receptor ligand has yet been reported (Nelson, 1993).

* Corresponding author. Institute de Recherche Jouveinal, 3–9 rue de la Loge, 94265 Fresnes, France. Tel.: (33) (1) 4096-7478; fax: (33) (1) 4096-7559.


*PII* S0014-2999(96)00180-X

The 5-$HT_{2C}$ receptor antagonist, SB 200646 (*N*-(1-methyl-5-indolyl)-*N'*-(3-pyridyl)urea), also inhibits $5HT_{2B}$ receptor mediated responses in the rat stomach fundus (Forbes et al., 1993). Another antagonist, ritanserin, has high affinities for human 5-$HT_{2A}$, rat and mouse 5-$HT_{2B}$, rat 5-$HT_{2C}$, rat 5-$HT_6$, rat, mouse and human 5-$HT_7$ (Boess and Martin, 1994) and rat dopamine $D_2$ receptors (Van Wijngaarden et al., 1990).

The superfamily of G-protein-coupled receptors has been divided into five families (Kolakowski, 1994). Family A includes opsins, odorant receptors and receptors for various endogenous ligands, including biogenic amines, neuropeptides, glycoprotein hormones, platelet activating factor, thrombin, adenosine, nucleotides and eicosanoids. The transmembrane segments in the amino-acid sequences of G-protein-coupled receptors have been located by mapping of extracellular and intracellular domains by peptide-specific antibodies (Wang et al., 1989), calculation of hydrophobic indices, combined analysis of hydrophobicity and distribution of charged residues, analysis of $\alpha$-helix periodicity (hydrophobicity or conservation) and by analysis of occurrence of non-conserved Pro residues (Ballesteros and Weinstein, 1994). Many of the three-dimensional models of G-protein-coupled receptors, including several 5-$HT_{2A}$ receptor models, which have been proposed (Trumpp-Kallmeyer et al., 1992; Westkaemper and Glennon, 1993; Choudhary et al., 1995) have used a model of bacteriorhodopsin (Henderson et al., 1990) as a template for the seven transmembrane helices. This method has been questioned, due to the low sequence similarities between bacteriorhodopsin and G-protein-coupled receptors (Pardo et al., 1992). Models of G-protein-coupled receptors that use the bacteriorhodopsin as a rigid structure template are likely to ignore residues on transmembrane helix 7, especially those with small side-chains, since they are relatively distant from the other known ligand binding residues on transmembrane helices 3, 5 and 6 (Donnelly et al., 1994).

In the present study, a three-dimensional model of the rat 5-$HT_{2C}$ receptor was constructed from its amino-acid sequence (Julius et al., 1990), by molecular modeling techniques. An arrangement of the seven transmembrane helices as suggested by the projection map of bovine rhodopsin (Schertler et al., 1993; Baldwin, 1993) was chosen rather than the bacteriorhodopsin model, due to the sequence similarity between rhodopsin and G-protein-coupled neurotransmitter receptors. The transmembrane helices were assembled in an anticlockwise arrangement, viewed from the extracellular side. Residues that were conserved in more than 50% out of 105 different G-protein-coupled receptors (Baldwin, 1993), belonging to the A family, and residues involved in ligand binding to other family A G-protein-coupled receptors according to site-directed mutagenesis studies, were oriented towards a central core between the transmembrane helices. The receptor model was used to examine receptor interactions of serotonin, ketanserin and ritanserin (Fig. 1), to identify residues involved in the binding of each ligand and to simulate the molecular dynamics of receptor–ligand interactions.

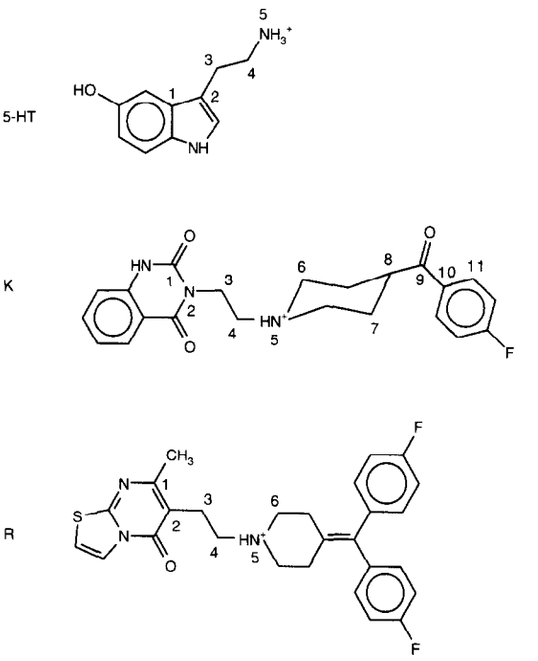


Fig. 1. Structure of protonated serotonin (5-HT), ketanserin (K) and ritanserin (R). Torsional angles: T1, 1–2–3–4; T2: 2–3–4–5; T3: 3–4–5–6; T4: 7–8–9–10; T5: 8–9–10–11.

## 2. Materials and methods

### 2.1. Computational procedures

The united atom force field (Weiner et al., 1984) of the AMBER 4.0 programs (Pearlman et al., 1991) was used for molecular mechanics calculations and molecular dynamics simulations. The calculations were done on Sun SPARCstation 1, Sun SPARCstation 2 and CRAY Y-MP4D/464 computers. The parameters used for energy minimization and molecular dynamics simulation are summarized in Table 1. United atom parameters and net

Table 1
Parameters used in molecular mechanics energy minimization (EM) and molecular dynamics simulations (MD)

| | EM | MD |
|---|---|---|
| Scale factor 1–4, van der Waals interactions | 8 | 8 |
| Scale factor 1–4, electrostatic interactions | 2 | 2 |
| Cut-off radius, non-bonded interactions | 10 Å | 10 Å |
| Steps between updating of non-bonded pair list | 25 | 25 |
| Step length (initial in EM) | 0.005 | 0.001 ps |
| Dielectric function | $\epsilon = r$ | $\epsilon = r$ |
| Temperature | | 310 K |
| Constraints | | all bond lengths |
| Time between saving of coordinates | | 1 ps |

atomic charges for serotonin, ritanserin and ketanserin had been developed previously (Edvardsen et al., 1992; Kristiansen et al., 1993). Individual transmembrane helices were energy-minimized by 10 steps of steepest descent minimization and 90 steps of conjugate gradient minimization, which was repeated until convergence with an 0.02 kcal $mol^{-1}$ root mean square energy gradient difference between successive steps (Table 1). Energy minimization of receptor models and of ligand–receptor complexes before the simulations, were performed by 500 steps of steepest descent minimization followed by 2000 steps of conjugate gradient minimization. Energy minimization of ligand–receptor complexes after the simulations were performed by 500 steps of steepest descent minimization followed by conjugate gradient minimization until convergence with a 0.02 kcal $mol^{-1}$ $Å^{-1}$ root mean square energy gradient difference between successive minimization steps. The MidasPlus programs (Ferrin et al., 1988) were used for molecular graphics on a Silicon Graphics Indigo$^2$ Extreme work station. The MIDAS programs (Ferrin et al., 1988) were used to calculate water-accessible surfaces and molecular electrostatic potentials 1.4 Å outside the surfaces, with a distance-dependent dielectric function and a 12-Å cut-off radius for non-bonded interactions.

### 2.2. Receptor modeling

Sequence alignment and average hydropathy indices of 14 biogenic amine neurotransmitter receptors were previously used to localize the seven transmembrane segments in various G-protein-coupled receptors, including the rat 5-$HT_{2C}$ receptor (Dahl et al., 1991), assuming a 27 residue length of each transmembrane helix. These localizations of transmembrane helices were used in the present model. The start- and end-points of each transmembrane helix are indicated in Table 2.

Computer graphics techniques were used to build models of each of the seven transmembrane helices of the rat 5-$HT_{2C}$ receptor from the amino-acid sequence (Julius et al., 1990). Units up to pentapeptide size containing a proline residue were assigned backbone torsional angles ($\phi$, $\psi$ and $\omega$) using the $Ala^{120}$-$Phe^{121}$-$Cys^{122}$-$Val^{123}$-$Pro^{124}$ segment of helix C in the L subunit of the crystal structure of the photosynthetic reaction center of *Rhodopseudomonas viridis* (Deisenhofer and Michel, 1989) as a template. This introduced kinks in the helical axis in stretches preceding prolines. All the other transmembrane residues were assigned $\phi = -57°$, $\psi = -47°$ and $\omega = 180°$ torsional angles, corresponding to an idealized $\alpha$-helix, in the initial models of each helix. Each of the transmembrane helices were energy-minimized, and water-accessible surfaces and molecular electrostatic potentials were calculated for each of the energy-minimized helices.

Interactive computer graphics were used to assemble the seven $\alpha$-helices into an antiparallell arrangement, anticlockwise when viewed from the extracellular side, approximately corresponding to a projection map of bovine rhodopsin (Schertler et al., 1993). Various single-point mutations of transmembrane residues in G-protein-coupled receptors have been reported to affect ligand binding affinities. The corresponding residues in the rat 5-$HT_{2C}$ receptor were identified from sequence alignments, and transmembrane helices 2–7 were oriented such that these residues were facing the central core between the transmembrane helices. Helix 1 was rotated such that the most negative electrostatic potentials, which were around $Thr^{68}$ and $Asn^{72}$, faced the central core between the helices. All the helices were initially placed with their axis approximately perpendicular to the membrane surface.

The loops between transmembrane helices, N- and C-terminals were built with secondary structures according to Garnier Robson predictions (Garnier et al., 1978). The $\phi$ and $\psi$ torsional angles in residues predicted in random coil conformations were rotated in order to position the ends of the loops and terminals near the ends of transmembrane helices.

Site-directed mutagenesis experiments with various G-protein-coupled receptors have suggested that a disulfide bond between a cysteine residue in the first extracellular loop or near the extracellular end of transmembrane helix 3 and a cysteine in the second extracellular loop may be conserved among many G-protein-coupled receptors (Baldwin, 1993). A disulfide bond between $Cys^{128}$ and $Cys^{208}$ was, therefore, included in the 5-$HT_{2C}$ receptor model.

### 2.3. Refinement of receptor models

The loops, N- and C-terminals, including the disulfide bridge between $Cys^{128}$ and $Cys^{208}$, were energy-minimized while the other parts of the transmembrane helices were kept in fixed positions. The whole receptor model was then

Table 2
Localization of segments in the rat 5-$HT_{2C}$ receptor model

| Domain | Residues |
|---|---|
| N-terminal | $Met^{1}$-$Val^{53}$ |
| TMH [a] 1 | $Gln^{54}$-$Ser^{80}$ |
| Intracellular loop 1 | $Met^{81}$-$Thr^{89}$ |
| TMH 2 | $Asn^{90}$-$Leu^{116}$ |
| Extracellular loop 1 | $Tyr^{117}$-$Leu^{123}$ |
| TMH 3 | $Pro^{124}$-$Ser^{150}$ |
| Intracellular loop 2 | $Leu^{151}$-$Thr^{170}$ |
| TMH 4 | $Lys^{171}$-$Asp^{197}$ |
| Extracellular loop 2 | $Glu^{198}$-$Asp^{212}$ |
| TMH 5 | $Pro^{213}$-$Ile^{239}$ |
| Intracellular loop 3 | $Tyr^{240}$-$Ser^{312}$ |
| TMH 6 | $Lys^{313}$-$Cys^{339}$ |
| Extracellular loop 3 | $Gly^{340}$-$Leu^{347}$ |
| TMH 7 | $Met^{348}$-$Asn^{374}$ |
| C-terminal | $Lys^{375}$-$Val^{460}$ |

[a] TMH, transmembrane helix.

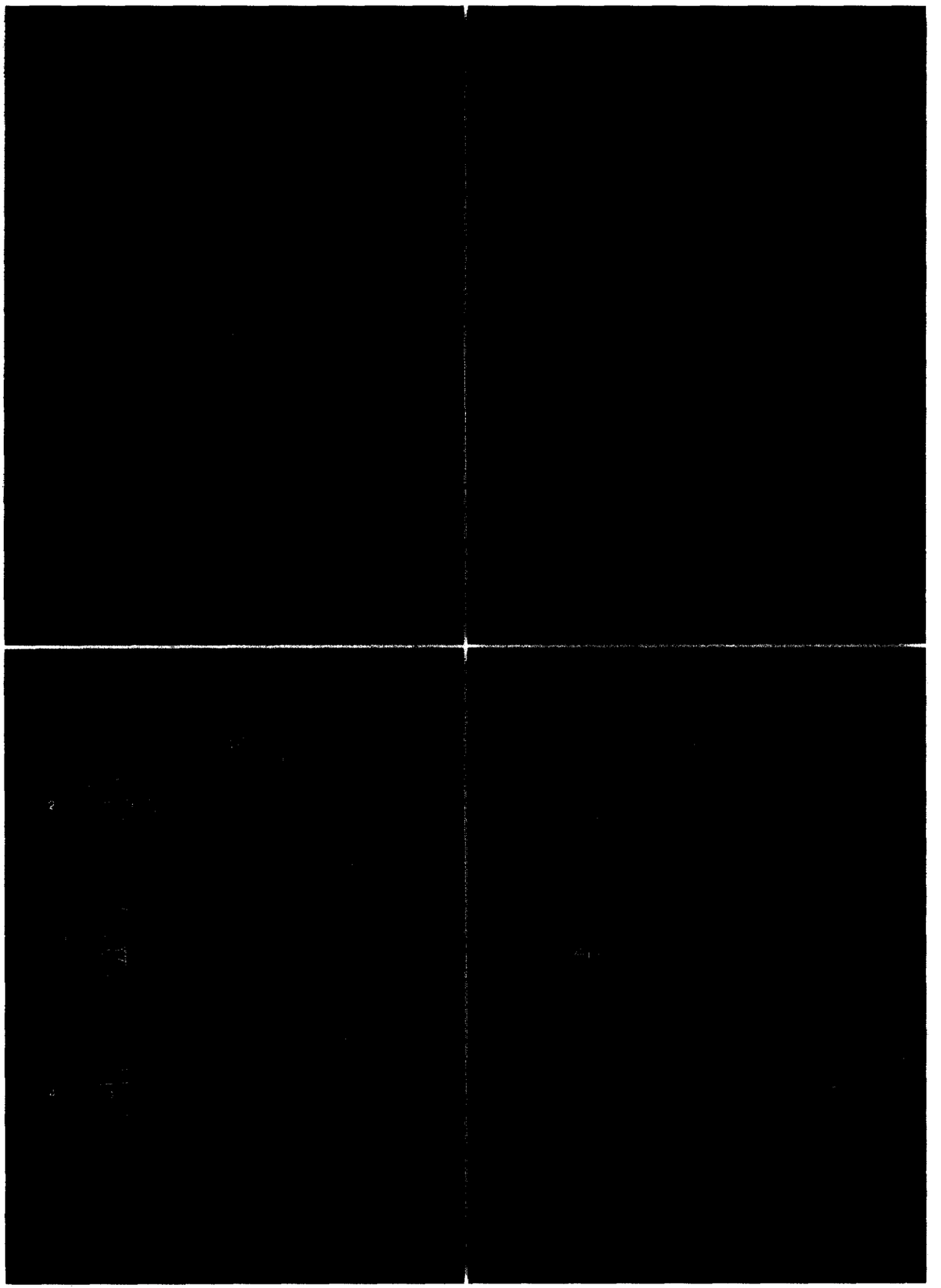

refined by energy minimization. Loops, N- and C-terminals and the cysteine bridge were further refined by a 20-ps molecular dynamics simulation, where the transmembrane helices not were allowed to move, followed by energy minimization of the whole receptor model. Transmembrane helices 4 and 5 in this model were rotated around their axis by interactive computer graphics, such that 32 out of the 36 residues in transmembrane helices 1–7 that were conserved in more than 50% of 105 different family A G-protein-coupled receptor sequences (Baldwin, 1993), were oriented towards the central core of the receptor model and the model was energy-minimized. The model was further refined by 20 ps of molecular dynamics simulation of loops and terminals, followed by energy minimization of the whole model. The water-accessible surface and molecular electrostatic potentials of the receptor model were then calculated.

### 2.4. Ligand–receptor interactions

United atomic models of serotonin, ritanserin and ketanserin had previously been constructed (Edvardsen et al., 1992; Kristiansen et al., 1993). The torsional angles defining the ligand conformations are indicated in Fig. 1. Serotonin was initially docked into the receptor model, close to transmembrane helices 5 and 6. Ketanserin and ritanserin were docked into the model in two different orientations each, one with the fluoro group(s) directed towards the extracellular side and one with the fluoro group(s) towards the intracellular side, always with the protonated amine group close to the carboxylate group of $Asp^{135}$ in transmembrane helix 3. The initial ligand–receptor complexes were energy-minimized and used as start structures for 41 ps of molecular dynamics simulations, which seems to be sufficient to examine receptor–ligand interactions in such models (Edvardsen et al., 1992). The structures observed after 20 ps and the final structures from the simulations were energy-minimized and ligand interactions with individual amino-acid residues were calculated. One 41-ps simulation of the receptor model without any ligand was also performed. An alignment (Oliveira et al., 1993), which includes 730 receptor sequences, has been used in the present study in order to find out whether particular amino-acid residues are conserved among the whole family A of G-protein-coupled receptors, among biogenic amine receptors, among serotonin receptors or among 5-$HT_2$ receptor subtypes.

## 3. Results

### 3.1. Receptor modeling

The initial receptor model is shown in Fig. 2. The molecular electrostatic potentials were mainly positive in the cytoplasmic parts and negative in the extracellular parts of the receptor model, both before and after molecular dynamics simulations, as shown in Fig. 2 for the initial model. Areas in the central core around $Asp^{100}$ in transmembrane helix 2 and $Asp^{135}$ in transmembrane helix 3 had particularly low electrostatic potentials. There were 5 positively charged residues (Lys, Arg) in the extracellular, 6 in the transmembrane and 38 in the intracellular domains, and 7 negatively charged residues (Asp, Glu) in the extracellular, 4 in the transmembrane and 22 in the intracellular domains of the receptor model, as indicated in the upper right part of Fig. 2.

Site-directed mutagenesis studies have identified 52 different residues within the transmembrane helices of family A G-protein-coupled receptors that may be involved in ligand binding (Baldwin, 1993, 1994). Among the 52 corresponding residues in the rat 5-$HT_{2C}$ receptor (Table 3), 36 were located in the central core between transmembrane helices, as shown in the lower left part of Fig. 2. The other 16 residues, on the membrane facing side, were $Leu^{102}$, $Leu^{105}$, $Val^{107}$ and $Leu^{112}$ in transmembrane helix 2, $Val^{136}$ and $Leu^{137}$ in transmembrane helix 3, $Ala^{177}$ and $Leu^{195}$ in transmembrane helix 4, $Phe^{221}$ in transmembrane helix 5, $Ile^{324}$, $Met^{325}$, $Cys^{327}$, $Pro^{328}$ and $Ser^{332}$ in transmembrane helix 6, $Val^{361}$ and $Thr^{371}$ in transmembrane helix 7. Mutations of such residues, which are on the membrane facing side of the helices, may change the local structure of the ligand binding site, and thereby ligand binding affinities and capacities.

Among the 39 residues within the transmembrane domains (Table 3) that are conserved in more than 50% of 105 different family A G-protein-coupled receptors (Baldwin, 1993), only 4 ($Ser^{95}$ in transmembrane helix 2, $Pro^{328}$, $Met^{325}$ in transmembrane helix 6 and $Ile^{358}$ in transmembrane helix 7) were on the membrane facing side of the transmembrane helices in the present receptor model (Fig. 2, lower right part). Most of these conserved residues were located in the half of the transmembrane helices closest to the cytoplasmic membrane surface. Exceptions were $Pro^{189}$ in transmembrane helix 4, $Phe^{224}$ in transmembrane helix 5, $Pro^{328}$ and $Phe^{329}$ in transmembrane

Fig. 2. Top: initial receptor model before simulations, viewed in the membrane plane. Left: water accessible molecular surface, color coded according to electrostatic potentials. Blue: $e < -20.0$ kcal $mol^{-1}$, white: $-20.0 \leq e \leq 20.0$ kcal $mol^{-1}$, red: 20.0 kcal $mol^{-1} < e$. Right: $C_\alpha$ chain. Red: positively charged residues (Arg and Lys). Blue: negatively charged residues (Asp and Glu). Bottom: $C_\alpha$ chains of transmembrane helices in the initial receptor model, viewed from the extracellular side. Left: Colored residues correspond to residues in other family A G-protein coupled receptors that may take part in ligand binding (Table 3). Right: Residues conserved in more than 50% of 105 different G-protein coupled receptors (Baldwin, 1993) (Table 3). Blue: $Asp^{100}$ in transmembrane helix 2 and $Asp^{135}$ in transmembrane helix 3. Green: Val, Leu, Ala, Met, Ile, Trp, Phe, Pro and Gly (hydrophobic). Yellow: Asn, Ser, Tyr, Thr and Cys (polar). Red: Lys and Arg.

Table 3
Residues in the rat 5-$HT_{2C}$ receptor corresponding to (A) residues in other family A G-protein coupled receptors that may take part in ligand binding according to site-directed mutagenesis experiments and (B) residues conserved in more than 50% of 105 different G-protein coupled receptors (Baldwin, 1993)

| Domain | Residues in the rat 5-$HT_{2C}$ receptor | |
|---|---|---|
| | A | B |
| TMH [a] 1 | | $Gly^{71}$, $Asn^{72}$, $Val^{75}$ |
| TMH 2 | $Asp^{100}$, $Leu^{102}$, $Val^{103}$, $Leu^{105}$, $Val^{107}$, $Ser^{111}$, $Leu^{112}$, $Ala^{114}$ | $Asn^{90}$, $Leu^{93}$, $Ser^{95}$, $Leu^{96}$, $Ala^{97}$, $Ala^{99}$, $Asp^{100}$, $Met^{101}$ |
| TMH 3 | $Cys^{128}$, $Pro^{129}$, $Trp^{131}$, $Asp^{135}$, $Val^{136}$, $Leu^{137}$, $Phe^{138}$, $Ser^{139}$ | $Cys^{128}$, $Ser^{142}$, $Leu^{146}$, $Ile^{149}$, $Ser^{150}$ |
| Intracellular loop 2 | | $Asp^{152}$, $Arg^{153}$, $Tyr^{154}$ |
| TMH 4 | $Ala^{177}$, $Trp^{180}$, $Val^{186}$, $Pro^{189}$, $Leu^{195}$, $Arg^{196}$ | $Trp^{180}$, $Ser^{183}$, $Pro^{189}$ |
| TMH 5 | $Val^{216}$, $Gly^{219}$, $Ser^{220}$, $Phe^{221}$, $Ala^{223}$, $Phe^{224}$, $Pro^{227}$, $Leu^{237}$ | $Phe^{224}$, $Pro^{227}$, $Met^{231}$, $Tyr^{235}$, $Thr^{238}$ |
| TMH 6 | $Phe^{322}$, $Ile^{324}$, $Met^{325}$, $Trp^{326}$, $Cys^{327}$, $Pro^{328}$, $Phe^{329}$, $Phe^{330}$, $Thr^{332}$, $Asn^{333}$, $Ser^{336}$, $Val^{337}$ | $Lys^{313}$, $Phe^{322}$, $Met^{325}$, $Trp^{326}$, $Pro^{328}$, $Phe^{329}$ |
| TMH 7 | $Leu^{352}$, $Phe^{355}$, $Val^{356}$, $Gly^{359}$, $Tyr^{360}$, $Val^{361}$, $Ser^{363}$, $Gly^{364}$, $Pro^{367}$, $Thr^{371}$ | $Ile^{358}$, $Cys^{362}$, $Ser^{363}$, $Asn^{366}$, $Pro^{367}$, $Tyr^{370}$ |

[a] TMH, transmembrane helix.

helix 6 and $Ile^{358}$ in transmembrane helix 7, all of which were in the half of transmembrane helices closest to the extracellular membrane surface. The conserved residues $Asp^{152}$, $Arg^{153}$ and $Tyr^{154}$ were situated in the second intracellular loop near transmembrane helix 3 outside the transmembrane helix domains.

The initial energy-minimized receptor model had a hydrogen bond between the $NH_2$ group of $Asn^{72}$ in transmembrane helix 1 and the carboxylate group of $Asp^{100}$ in transmembrane helix 2. In the final structure obtained after simulation and and energy minimization, the carboxylate group of $Asp^{100}$ in transmembrane helix 2 was hydrogen bonded to the side-chains of $Asn^{72}$ in transmembrane helix 1, $Asn^{366}$ and $Tyr^{370}$ in transmembrane helix 7, and the hydroxyl group of $Ser^{142}$ in transmembrane helix 3 was hydrogen-bonded to the $NH_2$ group of $Asn^{366}$ in transmembrane helix 7. The side-chains of these highly conserved residues formed a hydrophilic cavity between the transmembrane helices.

### 3.2. Ligand–receptor interactions

At the start of molecular dynamics simulations, the ligand–receptor models were heated from 0.1 to 310 K within 2 ps. In the energy-minimized serotonin–receptor complexes obtained during simulation 1, the root mean square difference of the backbone atom coordinates of the seven transmembrane helices was 3.57 between the 0- and 20-ps structures and 1.41 between the 20- and 41-ps structures. This shows that the most substantial structural changes took place within the first 20 ps of the simulations, as was generally the case in the simulations. The energy-minimized ligand–receptor complexes had from 39.4 to 72.4 kcal $mol^{-1}$ lower ligand–receptor interaction energies after 41 ps of simulation than before the simulation (Table 4).

The conformations of the ligand molecule (Table 4), ligand–residue interaction energies (Table 5), helix–helix interactions and the kinking of helices during the simulations were highly dependent on the initial position of the ligand. The final ligand conformations after 41 ps of molecular dynamics simulation of ligand–receptor complexes were in general very much dependent on the starting ligand conformations. Taken ketanserin as an example it was seen that the final conformation after 41 ps was hardly different from the starting structure as judged from T1-T5 in Table 4. A 41-ps molecular simulation from an initial ketanserin–receptor complex, with ketanserin in a (T1: −anti clinal, T2: anti periplanar, T3: +syn clinal, T4: −anti clinal) conformation and with the fluoro group closest to the intracellular side, produced more substantial changes in the ketanserin conformation (data not shown). During this simulation, T3 changed from a + syn clinal to an anti periplanar conformation. Table 5 shows ligand interaction energies with individual residues after 41 ps of simulation and energy minimization. $Asp^{135}$ in transmembrane helix 3 interacted more strongly with the ligand than did any other residue, during all simulations.

Table 6 identifies intramolecular hydrogen bonds in the receptor model after 41 ps of simulation and energy minimization. After 4 out of 6 simulations with a ligand, there were hydrogen bonds between the carboxylate group of $Asp^{100}$ in transmembrane helix 2 and both $Asn^{72}$ in transmembrane helix 1 and $Asn^{366}$ in transmembrane helix 7. The residues that formed these intramolecular hydrogen bonds did not interact with serotonin. However, some of

Table 4
Potential energies of ligands (L) and receptor models (R), ligand–receptor interaction energies (I) and torsional angles (T1-T5) of ligands in energy-minimized ligand–receptor complexes

| Ligand | Simulation | | Energy (kcal $mol^{-1}$) | | | Torsional angle (°) | | | | |
|---|---|---|---|---|---|---|---|---|---|---|
| | | | L | R | I | T1 | T2 | T3 | T4 | T5 |
| Serotonin | 1 | 0 ps | −6.3 | −9510 | −63.7 | 333.7 | 77.3 | | | |
| | | 20 ps | −3.2 | −10053 | −117.4 | 221.0 | 67.6 | | | |
| | | 41 ps | −3.8 | −10156 | −121.2 | 238.6 | 62.9 | | | |
| | 2 | 0 ps | −8.4 | −9511 | −56.7 | 293.2 | 68.7 | | | |
| | | 20 ps | −5.8 | −10003 | −91.2 | 279.9 | 45.8 | | | |
| | | 41 ps | −1.1 | −10118 | −101.1 | 280.3 | 282.0 | | | |
| Ketanserin | 1 | 0 ps | −36.8 | −9508 | −79.3 | 275.0 | 296.3 | 168.6 | 191.5 | 182.6 |
| | | 20 ps | −34.0 | −9940 | −126.7 | 289.5 | 305.9 | 173.6 | 207.8 | 172.1 |
| | | 41 ps | −36.1 | −10070 | −118.7 | 294.6 | 305.9 | 172.4 | 230.2 | 171.5 |
| | 2 | 0 ps | −35.4 | −9517 | −74.0 | 289.4 | 286.4 | 148.3 | 236.1 | 182.2 |
| | | 20 ps | −33.4 | −10062 | −130.8 | 288.5 | 286.9 | 166.9 | 230.1 | 183.4 |
| | | 41 ps | −35.2 | −10177 | −129.3 | 280.7 | 298.0 | 171.2 | 275.3 | 196.4 |
| Ritanserin | 1 | 0 ps | −19.2 | −9515 | −47.6 | 244.5 | 283.6 | 156.5 | | |
| | | 20 ps | −7.2 | −10065 | −118.2 | 144.5 | 300.2 | 140.5 | | |
| | | 41 ps | −9.8 | −10176 | −120.0 | 130.8 | 290.8 | 146.0 | | |
| | 2 | 0 ps | −11.3 | −9520 | −80.9 | 282.9 | 300.2 | 161.5 | | |
| | | 20 ps | −10.5 | −9994 | −118.5 | 276.4 | 300.9 | 170.1 | | |
| | | 41 ps | −9.6 | −10069 | −125.2 | 278.9 | 304.0 | 181.9 | | |

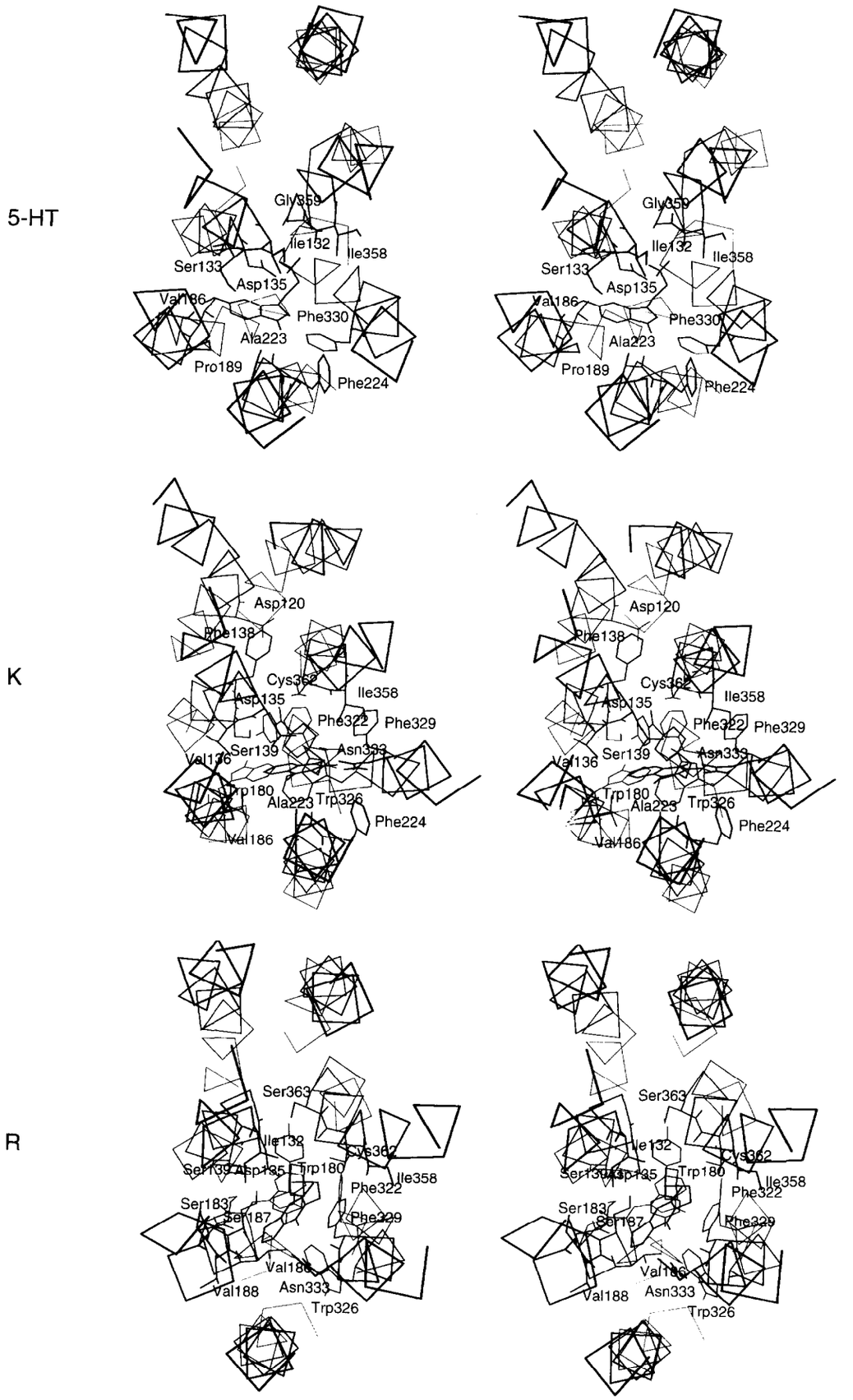
5-HT
Gly359
Ile132
Ile358
Ser133
Asp135
Val186
Phe330
Ala223
Pro189
Phe224
K
Asp120
Phe138
Cys362
Asp135
Ile358
Phe322
Phe329
Ser139
Asn333
Val136
Trp180
Ala223
Trp326
Phe224
Val186
R
Ser363
Ile132
Cys362
Ser130
Asp135
Trp180
Ile358
Phe322
Ser183
Ser187
Phe329
Val186
Val188
Asn333
Trp326

Table 5
Ligand interaction energies with individual residues ($\geq 2.0$ kcal mol$^{-1}$ or $\leq -2.0$ kcal mol$^{-1}$) after 41 ps of molecular dynamics simulation and energy minimization

| Residue | TMH [a] | Interaction energy (kcal mol$^{-1}$) | | | | | |
|---|---|---|---|---|---|---|---|
| | | Serotonin | | Ketanserin | | Ritanserin | |
| | | Sim. 1 | Sim. 2 | Sim. 1 | Sim. 2 | Sim. 1 | Sim. 2 |
| TMH 1, total | 1 | 0.0 | 0.0 | −0.1 | 0.0 | 0.0 | −0.1 |
| $Asp^{100}$ | 2 | | | | −2.0 | | |
| TMH 2, total | | 0.0 | 0.1 | −2.0 | −2.2 | −0.1 | −2.2 |
| $Cys^{128}$ | 3 | | | | | −2.8 | |
| $Trp^{131}$ | | | | −3.9 | | −7.9 | |
| $Ile^{132}$ | | −13.4 | −15.1 | −6.1 | | −4.1 | −2.7 |
| $Ser^{133}$ | | −2.8 | −5.9 | | | | |
| $Asp^{135}$ | | −51.8 | −38.0 | −49.5 | −54.0 | −46.2 | −43.0 |
| $Val^{136}$ | | | | | −2.1 | | |
| $Phe^{138}$ | | | | | −2.3 | | |
| $Ser^{139}$ | | | | | −3.8 | | −3.7 |
| TMH 3, total | | −71.1 | −60.3 | −63.7 | −68.2 | −63.5 | −56.6 |
| $Trp^{180}$ | 4 | | | | −2.6 | | −8.7 |
| $Ser^{183}$ | | | | −2.0 | | | −2.3 |
| $Val^{186}$ | | −8.6 | | | −2.3 | | −2.8 |
| $Ser^{187}$ | | | | | | | −2.8 |
| $Val^{188}$ | | | | | | | −2.6 |
| $Pro^{189}$ | | −2.0 | | | | −3.2 | |
| $Ile^{193}$ | | | | | | −3.1 | |
| $Arg^{196}$ | | | | 2.0 | | 2.8 | |
| $Asp^{197}$ | | | −2.2 | −2.1 | | −6.1 | |
| TMH 4, total | | −13.9 | −2.4 | −7.3 | −10.0 | −16.2 | −24.7 |
| $Ser^{220}$ | 5 | | −8.0 | | | | |
| $Ala^{223}$ | | −6.7 | | | −4.8 | −2.5 | |
| $Phe^{224}$ | | −2.0 | −2.0 | | −2.3 | | |
| $Ile^{226}$ | | | | | | −2.1 | |
| $Pro^{227}$ | | | | | | −3.4 | |
| TMH 5, total | | −11.2 | −13.4 | −4.2 | −11.7 | −11.7 | −1.3 |
| $Phe^{322}$ | 6 | | | | −3.5 | | −2.3 |
| $Trp^{326}$ | | | | −4.8 | −6.5 | −4.0 | −2.5 |
| $Phe^{329}$ | | | | −2.8 | −2.1 | −2.4 | −8.1 |
| $Phe^{330}$ | | −2.2 | | −6.1 | | | |
| $Asn^{333}$ | | | −7.8 | −3.2 | −8.3 | | −2.0 |
| TMH 6, total | | −6.4 | −8.9 | −18.9 | −25.1 | −12.4 | −20.7 |
| $Leu^{352}$ | 7 | | | −2.0 | | | |
| $Val^{354}$ | | | −2.0 | | | | |
| $Phe^{355}$ | | | −14.5 | −7.3 | | | |
| $Val^{356}$ | | | | −2.5 | | | |
| $Ile^{358}$ | | −12.0 | 2.2 | −3.0 | −3.7 | | −3.0 |
| $Gly^{359}$ | | −3.0 | | −2.0 | | | |
| $Cys^{362}$ | | | | | −2.6 | | −4.6 |
| $Ser^{363}$ | | | | | | | −4.0 |
| TMH 7, total | | −18.7 | −16.8 | −21.7 | −12.1 | −5.1 | −9.6 |
| All TMHs [b] | 1–7 | −121.2 | −101.1 | −118.7 | −129.3 | −120.0 | −125.2 |

[a] TMH, transmembrane helix; [b] TMHs, transmembrane helices.

these residues interacted with antagonists. Ketanserin interacted with $Asp^{100}$ and $Cys^{362}$ after simulation 2, ritanserin interacted with $Asp^{100}$, $Cys^{362}$ and $Ser^{363}$ after simulation 2.

Table 6
Intramolecular hydrogen bonds after 41 ps of simulation and energy minimization

| Ligand | Simulation | Intramolecular hydrogen bond | |
|---|---|---|---|
| Serotonin | 1 | $Asp^{100}(COO^-)$ | $Asn^{72}(NH_2)$ |
| | | $Asp^{100}(COO^-)$ | $Cys^{362}(SH)$ |
| | | $Asp^{100}(COO^-)$ | $Ser^{363}(OH)$ |
| | | $Asp^{100}(COO^-)$ | $Asn^{366}(NH_2)$ |
| | | $Tyr^{370}(OH)$ | $Asn^{366}(CO)$ |
| | | $Asp^{135}(COO^-)$ [a] | $Trp^{326}(NH)$ |
| | 2 | $Asp^{100}(COO^-)$ | $Asn^{72}(NH_2)$ |
| | | $Asp^{100}(COO^-)$ | $Tyr^{360}(OH)$ [b] |
| | | $Asp^{100}(COO^-)$ | $Ser^{363}(OH)$ |
| | | $Ser^{142}(OH)$ | $Asn^{366}(NH_2)$ |
| | | $Tyr^{370}(OH)$ | $Ser^{150}(OH)$ |
| Ketanserin | 1 | $Asp^{100}(COO^-)$ | $Asn^{72}(NH_2)$ |
| | | $Asp^{100}(COO^-)$ | $Ser^{363}(OH)$ |
| | 2 | $Asp^{100}(COO^-)$ | $Asn^{72}(NH_2)$ |
| | | $Asp^{100}(COO^-)$ | $Ser^{363}(OH)$ |
| | | $Asp^{100}(COO^-)$ | $Asn^{366}(NH_2)$ |
| Ritanserin | 1 | $Asp^{100}(COO^-)$ | $Asn^{72}(NH_2)$ |
| | | $Asp^{100}(COO^-)$ | $Ser^{363}(OH)$ |
| | | $Asp^{100}(COO^-)$ | $Asn^{366}(NH_2)$ |
| | | $Asn^{366}(NH_2)$ | $Ser^{142}(OH)$ |
| | 2 | $Asp^{100}(COO^-)$ | $Asn^{72}(NH_2)$ |
| | | $Asp^{100}(COO^-)$ | $Asn^{366}(NH_2)$ |
| | | $Asp^{100}(COO^-)$ | $Tyr^{370}(OH)$ |

[a] $Asp^{135}$ is conserved among biogenic amine receptors. [b] $Tyr^{360}$ is conserved among serotonin receptors.

### 3.3. Serotonin–receptor interactions

Serotonin had van der Waals contact with 15 different residues in transmembrane helices 3–7 after simulation 1. The OH group of serotonin interacted with the side-chain hydroxyl group of $Ser^{133}$ in transmembrane helix 3 and with the main-chain carbonyl group of $Val^{186}$ in transmembrane helix 4, and the indole NH group interacted with the main-chain carbonyl group of $Ala^{223}$ in transmembrane helix 5. The protonated amine group of serotonin was in close proximity to the carboxylate group of $Asp^{135}$ in transmembrane helix 3, the main-chain carbonyl groups of $Ile^{132}$ in transmembrane helix 3 and $Ile^{358}$ in transmembrane helix 7 (Fig. 3).

After simulation 2, serotonin had van der Waals contact with 11 different residues in transmembrane helices 3–7, and interactions with transmembrane helices 3 and 4 were 22.3 kcal mol$^{-1}$ weaker than after simulation 1 (Table 5). The protonated amine group of serotonin was near the carboxylate group of $Asp^{135}$ in transmembrane helix 3 and the main-chain carbonyl groups of $Phe^{355}$ and $Ile^{358}$ in transmembrane helix 7. The indole NH group in serotonin interacted with the side-chain hydroxyl group of $Ser^{133}$ in

Fig. 3. Stereo view of the $C_\alpha$ chains of transmembrane helices, the ligand and all amino acid residues having ligand interaction energy $\leq -2.0$ kcal mol$^{-1}$ in energy-minimized complexes after 41 ps molecular dynamics simulations, viewed from the extracellular side. 5-HT: Serotonin (simulation 1). K: Ketanserin (simulation 2); R: Ritanserin (simulation 2).

transmembrane helix 3. The OH group of serotonin was hydrogen-bonded to the side-chain OH group of $Ser^{220}$ in transmembrane helix 5 and to the side-chain $NH_2$ group of $Asn^{333}$ in transmembrane helix 6.

### 3.4. Ketanserin–receptor interactions

At the beginning of simulation 1, ketanserin was located between transmembrane helices 3, 6 and 7, with the *p*-fluoro-benzoyl towards the extracellular opening of the receptor model. In the energy-minimized ketanserin–receptor complexes, the ligand had van der Waals contact with 21 and 19 different residues in transmembrane helices 3–7 after 20 and 41 ps of simulation, respectively. Ketanserin had 8.0 kcal $mol^{-1}$ stronger receptor interaction energy after 20 ps than after 41 ps of simulation (Table 4). At the start of simulation 2, ketanserin was located between transmembrane helices 3, 6 and 7, with the quinazolindione moiety closest to the extracellular opening in the receptor model. After simulation and energy minimization, ketanserin had van der Waals contact with 22 different residues in transmembrane helices 3–7. There were strong aromatic–aromatic interactions between ketanserin and $Phe^{138}$ (transmembrane helix 3), $Trp^{180}$ in transmembrane helix 4, $Phe^{322}$, $Trp^{326}$ (transmembrane helix 6). The quinazolindione NH group was hydrogen-bonded to the side-chain carbonyl group of $Asn^{333}$ in transmembrane helix 6 (Figs. 3 and 4).

### 3.5. Ritanserin–receptor interactions

At the beginning of simulation 1, ritanserin was located between transmembrane helices 3–7 with the fluoro-benzene moieties oriented towards the extracellular opening of the binding pocket. After the simulation, ritanserin had van der Waals contact with 23 different residues in transmembrane helices (3–7) and with $Leu^{210}$, $Val^{209}$ and $Cys^{208}$ in the second extracellular loop. At the start of

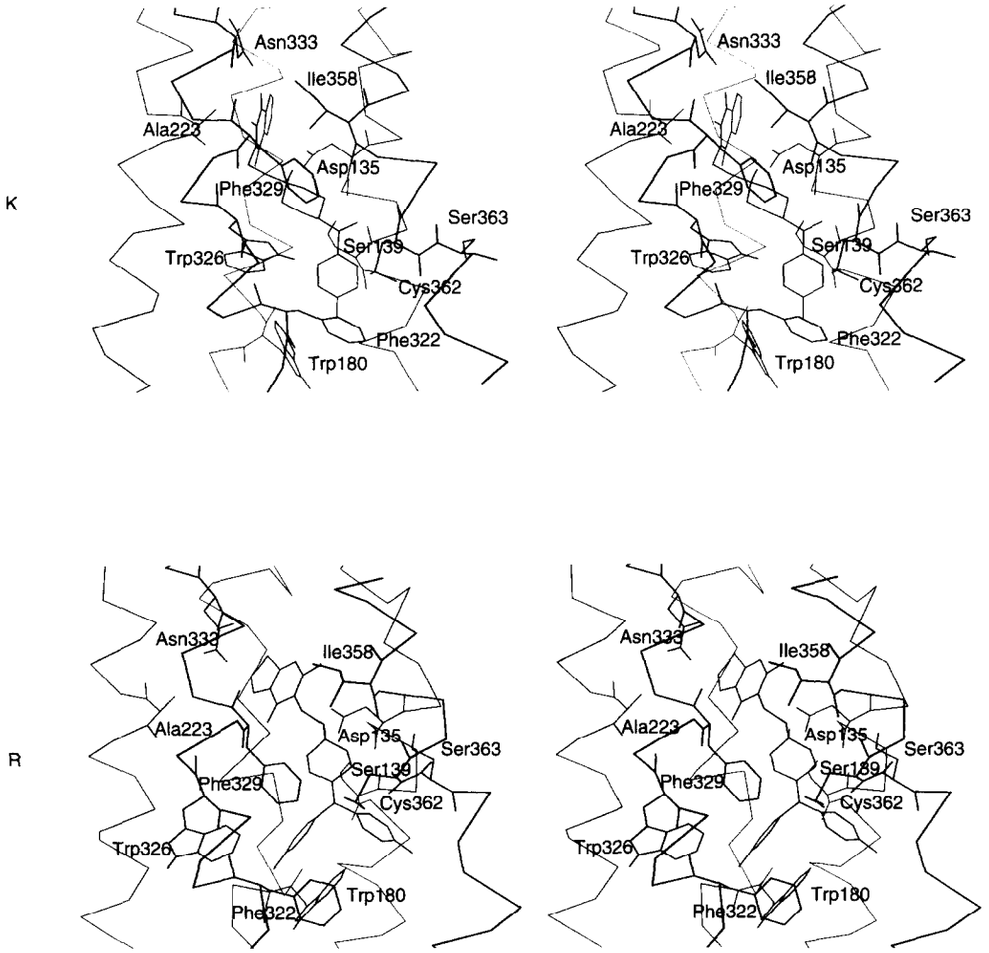


Fig. 4. Stereo view of the $C_\alpha$ chains of transmembrane helices 3–7, the ligand and some amino acid residues in energy-minimized complexes after 41 ps molecular dynamics simulations, viewed in the plane of the membrane bilayer with the extracellular side at the top of the figure. K: Ketanserin (simulation 2). R: Ritanserin (simulation 2). Amino acid residues displayed are those having ligand interaction energy $\leq -3.0$ kcal $mol^{-1}$ in one or both of the antagonist–receptor complexes shown in the figure.

simulation 2, ritanserin was located between transmembrane helices 3–7, with the fused ring system oriented towards the extracellular side of the receptor model. After the simulation, ritanserin had van der Waals contact with 26 different residues in transmembrane helices 3, 4, 6 and 7. There were strong aromatic–aromatic interactions between ritanserin and $Trp^{180}$ in transmembrane helix 4, $Phe^{322}$, $Trp^{326}$, $Phe^{329}$ (transmembrane helix 6) (Fig. 3). One of the two fluoro-benzene rings in ritanserin was stacked with the aromatic ring of $Trp^{180}$, and the other fluoro-benzene ring was approximately perpendicular to the indole ring of $Trp^{180}$ (Figs. 3 and 4).

## 4. Discussion

### 4.1. Ligand binding site

In the present study, interactions between the rat 5-$HT_{2c}$ receptor and three protonated ligands were examined using molecular dynamics simulations of ligand–receptor complexes. The simulations with the antagonists, ketanserin and ritanserin, oriented with the fluoro-benzene moiety towards the cytoplasmic opening of the central duct of the receptor model, produced the strongest ligand–receptor interactions (simulations 2 with antagonists). As seen from Table 4, both ketanserin and ritanserin stayed in (T1: −syn clinal, T2: −syn clinal, T3: anti periplanar) conformations during these simulations. After simulation 2 with ketanserin, the distance from the protonated piperidine nitrogen atom to the centroid of the benzoyl ring in ketanserin was 6.6 Å. This is close to the corresponding $6.4 \pm 0.4$ Å distance reported in a pharmacophore model derived from series of 5-$HT_{2A}$ receptor antagonists (Andersen et al., 1994).

Results with rat 5-$HT_{2A/2C}$ chimeric receptors suggest that structurally diverse 5-$HT_2$ receptor antagonists utilize different regions of the 5-$HT_{2A}$ receptor for high-affinity binding (Choudhary et al., 1992). Similar results were obtained in the present simulations of ligand–5-$HT_{2C}$ receptor complexes, suggesting that distinct domains may be involved in binding of serotonin, ketanserin and ritanserin. Among the transmembrane helices, transmembrane helix 3 interacted most strongly with the ligand molecule after all simulations (range: −56.6 kcal $mol^{-1}$ to −71.1 kcal $mol^{-1}$). After simulation 1 with serotonin, transmembrane helix 7 interacted very strongly with serotonin (−18.7 kcal $mol^{-1}$). After simulations 2 with antagonists, transmembrane helix 6 interacted very strongly with ketanserin (−25.1 kcal $mol^{-1}$) and ritanserin (−20.7 kcal $mol^{-1}$), whereas transmembrane helix 4 interacted very strongly (−24.7 kcal $mol^{-1}$) with ritanserin (Table 5).

Several site-directed mutagenesis experiments with various G-protein-coupled receptors for biogenic amines suggest that the conserved aspartic acid residue in transmembrane helix 3 ($Asp^{135}$ in the rat 5-$HT_{2C}$ receptor) is the primary counterion for the protonated amine group in antagonists and agonists (Wang et al., 1993). The single-point mutants $Asp^{120}Asn$ (transmembrane helix 2) and $Asp^{155}Asn$ (transmembrane helix 3) in the rat 5-$HT_{2A}$ receptor showed 10- and 75-fold decreases in ketanserin binding affinity, and 7- and 37-fold decreases in serotonin binding affinity, respectively, compared to the wild-type receptor (Wang et al., 1993). The present simulations of ligand–receptor complexes are in perfect agreement with these results, and suggest a particularly strong interaction between the ligand and $Asp^{135}$ in the 5-$HT_{2C}$ receptor. The varying functional effects of mutations at the conserved Asp residue in transmembrane helix 2 in different G-protein-coupled receptors suggest that this residue is involved in receptor rearrangement among different conformational states (Sealfon et al., 1995).

The present simulations do not, however, rule out the possibilities that other conformations of serotonin, ketanserin and ritanserin may bind to the 5-$HT_{2C}$ receptor, and to other sites on the receptor.

### 4.2. Antagonist binding selectivity

The radiolabeled 5-$HT_{2C}$ receptor has a pharmacological profile similar to that of the radiolabeled 5-$HT_{2A}$ receptor, with certain important exceptions (Nelson, 1993; Peroutka, 1994). Due to the 79% amino-acid identities in the transmembrane segments of these two receptor sequences (Nelson, 1993), it is very likely that compounds with high affinities at both subtypes share similar modes of receptor interaction at both subtypes. Whereas highly selective antagonists (Dudley et al., 1990; Herndon et al., 1992) and agonists (Glennon et al., 1994) for the 5-$HT_{2A}$ receptor have been developed, highly selective ligands for the 5-$HT_{2C}$ receptor remain to be discovered (Forbes et al., 1993; Nelson, 1993). The relatively high number of different types of chemical structures that have similar affinities for both these subtypes, and the high similarity in their amino-acid sequences, suggest that development of subtype selective compounds within the 5-$HT_2$ receptor subfamily will continue to be a challenge (Nelson, 1993). Three-dimensional models of complexes between ligands and 5-$HT_2$ receptors may provide novel insight into ligand–receptor interactions and suggest specific subtype and species differences in ligand binding affinities, which may be further examined by molecular biological techniques.

As shown in Figs. 3 and 4, $Cys^{362}$ in transmembrane helix 7 had van der Waals contact with the antagonist after simulation 2 with ketanserin and after simulation 2 with ritanserin. The majority of family A receptor sequences (69% of 730 sequences) (Oliveira et al., 1993) has an Asn residue in the position corresponding to $Cys^{362}$ in the 5-$HT_{2C}$ receptor, while the 5-$HT_{2A}$ and 5-$HT_{2B}$ receptors have a Ser residue in the corresponding position (Oliveira et al., 1993). We suggest, therefore, that the unique ligand binding profiles of 5-$HT_2$ receptors may depend on the

presence of a small polar residue at the position corresponding to $Cys^{362}$ in the 5-$HT_{2C}$ receptor. The 5-$HT_{2A}$, 5-$HT_{2B}$ and 5-$HT_{2C}$ receptors have an asparagine residue corresponding to $Asn^{333}$ (transmembrane helix 6) in the rat 5-$HT_{2C}$ receptor (Oliveira et al., 1993), which suggests that the ligand binding profile of 5-$HT_2$ receptors also may depend on this residue. The present models of antagonist–receptor complexes suggest that $Asn^{333}$ may form a hydrogen-bonding interaction, whereas $Ala^{223}$ may form a strong van der Waals interaction with the fused ring system in ketanserin, but not in ritanserin (Fig. 4). This is in accordance with results from ligand binding studies, suggesting that the nature of the piperidine nitrogen-substituent in ketanserin-related analogues may affect (1) the particular mode of 5-$HT_{2A}$ receptor binding for such compounds (Ismaiel et al., 1995) and (2) 5-$HT_{2A}$ vs. 5-$HT_{2C}$ receptor binding selectivity (Herndon et al., 1992).

A common structural feature among several antagonists showing selective binding to 5-$HT_{2A}$ vs. 5-$HT_{2C}$ receptors, is a reactive oxygen atom corresponding to the benzoyl oxygen atom in ketanserin (Pierce et al., 1992). According to the present model, the benzoyl carbonyl group in ketanserin may be in close proximity to $Ser^{139}$ (transmembrane helix 3), which is conserved among mammalian 5-$HT_{2A}$, 5-$HT_{2B}$, 5-$HT_{2C}$ receptors, and $Cys^{362}$ (transmembrane helix 7), which is not conserved (Fig. 4). A different hypothesis suggests that the ketanserin molecule is localized with its *p*-fluoro benzoyl moiety near the extracellular ends of the transmembrane helices (Pierce et al., 1992). According to this hypothesis, the benzoyl carbonyl group (or another reactive oxygen-containing group) in ketanserin-type compounds may interact with one or both of the non-conserved residues, $Ser^{336}$ or $Lys^{350}$, near the extracellular ends of transmembrane helices 6 and 7 of the rat 5-$HT_{2C}$ receptor. The 5-$HT_{2A}$ receptor has Ala residues, whereas the 5-$HT_{2B}$ receptor subtype has a Leu and a Thr/Met corresponding to these Ser and Lys residues in the 5-$HT_{2C}$ receptor (Oliveira et al., 1993). As a consequence of these interactions, the protonated piperidine NH group and the benzoyl moiety in such compounds may interact more weakly with residues in the 5-$HT_{2C}$ receptor than with residues in the 5-$HT_{2A}$ receptor. Others have proposed that the benzoyl carbonyl group in ketanserin-type compounds form a hydrogen bond with a residue in the 5-$HT_{2A}$ receptor (Andersen et al., 1994). We suggest that this hydrogen- bonding interaction may involve the serine residue in the 5-$HT_{2A}$ receptor, corresponding to $Cys^{362}$ in the rat 5-$HT_{2C}$ receptor, and that this Cys/Ser difference may contribute to subtype differences in ligand binding affinities between the 5-$HT_{2A}$ and 5-$HT_{2C}$ receptor subtypes. The present hypothesis and the hypothesis proposed by Pierce et al. (1992) are both in agreement with results from experiments with chimeric rat 5-$HT_{2A/2C}$ receptors, suggesting that important determinants for the selective binding of ketanserin to the 5-$HT_{2A}$ receptor are located in transmembrane helix 3 and in the C-terminal domains, including transmembrane helices 6 and 7 (Choudhary et al., 1992).

Molecular modeling of transmembrane helix bundles of 5-$HT_{2A}$, 5-$HT_{2B}$ and 5-$HT_{2C}$ receptors have identified 8 residues with various functional properties in the different 5-$HT_2$ receptor subtypes, which are located in the central cavity (Westkaemper and Glennon, 1993). Only 3 out of these 8 residues, corresponding to $Ser^{187}$ (transmembrane helix 4), $Met^{348}$ and $Glu^{349}$ (transmembrane helix 7) in the rat 5-$HT_{2C}$ receptor, were predicted to be localized near or at the putative ligand binding site in these receptor models (Westkaemper and Glennon, 1993). $Arg^{196}$ (Leonhardt et al., 1993), $Ser^{336}$, $Lys^{350}$ (Pierce et al., 1992), located near the extracellular ends of the transmembrane helices 4, 6 and 7 in the rat 5-$HT_{2C}$ receptor, are other non-conserved residues with differing functional groups, that have been proposed to be key residues determining subtype selectivity in ligand binding to 5-$HT_2$ receptor subtypes. According to the present simulations, three non-conserved residues with different functional groups, $Cys^{362}$ (transmembrane helix 7), $Ser^{133}$ (transmembrane helix 3), $Ser^{187}$ (transmembrane helix 4), may take part in ligand binding to the rat 5-$HT_{2C}$ receptor.

### 4.3. Agonist binding selectivity

Serotonin has significantly higher affinity for the agonist low-affinity state of the 5-$HT_{2C}$ receptor than for the corresponding state of the 5-$HT_{2A}$ receptor, while the difference was less pronounced for the agonist high-affinity states (Boess and Martin, 1994). Experiments with the single-point mutant $Arg^{195}Gln$ in the human 5-$HT_{2C}$ receptor have suggested that this Arg residue contributes to the higher affinity and potency of serotonin at the 5-$HT_{2C}$ receptor than at the 5-$HT_{2A}$ receptor (Leonhardt et al., 1993). In the present rat 5-$HT_{2C}$ receptor model, the corresponding $Arg^{196}$ residue was involved in a network of salt bridges involving $Arg^{125}$, $Asp^{197}$ and $Asp^{212}$ near the extracellular ends of transmembrane helices 3–5, respectively. Different residues with various functional properties are located at these positions in the different 5-$HT_2$ receptor subtypes. The 5-$HT_{2A}$ receptor has a Gln and the 5-$HT_{2B}$ receptor has a Glu residue, corresponding to $Arg^{196}$ in the rat 5-$HT_{2C}$ receptor (Oliveira et al., 1993). According to the present model, the $Arg^{195}Gln$ substitution may change helix–helix interactions between transmembrane helices 3, 4 and 5 and thereby also the geometry of the ligand binding site. In the present models, direct interactions between ligands and the side-chains of $Arg^{196}$ and $Asp^{197}$, at the extracellular opening in the duct formed by the seven transmembrane helices, were not observed.

### 4.4. The role of proline residues

Site-directed mutagenesis studies of the highly conserved proline residues in transmembrane helices 4–7 (Fig. 2) of the rat $m_3$ muscarinic receptor have suggested that

these are important for receptor expression, ligand binding and signal transduction (Wess et al., 1993). All G-protein-coupled serotonin receptors have prolines at positions corresponding to those of $Pro^{227}$, $Pro^{328}$, $Pro^{367}$, and proline(s) corresponding to one or both of $Pro^{189}$ and $Ile^{190}$ in the rat 5-$HT_{2C}$ receptor (Oliveira et al., 1993). Serotonin interacted with $Pro^{189}$ in transmembrane helix 4 after simulation 1, ritanserin interacted with $Pro^{189}$ and $Pro^{227}$ after simulation 1, whereas ketanserin did not interact with any of these two proline residues (Table 5). $Pro^{189}$ and $Pro^{227}$ also exposed the carbonyl groups of $Val^{186}$ in transmembrane helix 4 and $Ala^{223}$ in transmembrane helix 5 into the putative ligand binding pocket. As shown in Fig. 3, $Val^{186}$ and $Ala^{223}$ were hydrogen-bonded to serotonin after simulation 1. $Pro^{328}$ was on the membrane-facing side of transmembrane helix 6 in the receptor model (Fig. 2).

### 4.5. The role of aromatic residues

In addition to the prolines, 7 aromatic residues in the transmembrane domains of the 5-$HT_{2C}$ receptor ($Trp^{180}$ in transmembrane helix 4, $Phe^{224}$ and $Tyr^{235}$ in transmembrane helix 5, $Phe^{322}$, $Trp^{326}$ and $Phe^{329}$ in transmembrane helix 6 and $Tyr^{370}$ in transmembrane helix 7) are conserved in all G-protein-coupled serotonin receptors (Oliveira et al., 1993), and in more than 50% of 105 different family A G-protein-coupled receptors that have been cloned (Baldwin, 1993) (Fig. 2). 3 other aromatic residues in the transmembrane domains of the 5-$HT_{2C}$ receptor, $Phe^{330}$ in transmembrane helix 6, $Trp^{357}$ and $Tyr^{360}$ in transmembrane helix 7, are conserved in all G-protein-coupled serotonin receptors that have been cloned (Oliveira et al., 1993). It was interesting to note, therefore, that $Pro^{189}$, $Pro^{227}$ in transmembrane helix 5, and a cluster of 3 aromatic residues ($Phe^{224}$ in transmembrane helix 5, $Trp^{326}$ and $Phe^{330}$ in transmembrane helix 6) had van der Waals contact and formed a hydrophobic pocket around the indole ring of serotonin after simulation 1 (Fig. 3). The distance from the centroid of the benzene ring to the positively charged nitrogen atom in serotonin was 5.0 Å after simulation 1. According to a previous pharmacophore model derived from a series of 5-$HT_{2A}$ receptor agonists and structurally related antagonists, this distance should be approximately 5.1 (5.0–5.5) Å (Glennon et al., 1991).

The present simulations of serotonin–5-$HT_{2C}$ receptor complexes are in agreement with site-directed mutagenesis experiments suggesting that agonist binding and signal transduction in the 5-$HT_{2A}$ receptor require $Phe^{340}$ in transmembrane helix 6 but not $Phe^{339}$ in transmembrane helix 6 (corresponding to $Phe^{330}$ and $Phe^{329}$ in the rat 5-$HT_{2C}$ receptor), and that the opposite is the case for ketanserin binding (Choudhary et al., 1993; Choudhary et al., 1995). Different orientations of the ligand at the rat 5-$HT_{2A}$ receptor, at least with respect to $Phe^{340}$, have been proposed within closely related structure series of ergoline derivatives (Choudhary et al., 1995). Based on present findings, we propose that structural differences between ketanserin and ritanserin may give rise to different (overlapping) modes of binding of these two antagonists at the rat 5-$HT_{2C}$ receptor (Fig. 4). After simulation 2 with ketanserin, the aromatic $Phe^{138}$ (transmembrane helix 3), $Trp^{180}$ (transmembrane helix 4), $Phe^{322}$, $Trp^{326}$ (transmembrane helix 6) surrounded the fluoro-benzene moiety in ketanserin, whereas $Trp^{180}$ (transmembrane helix 4), $Phe^{322}$, $Trp^{326}$, $Phe^{329}$ (transmembrane helix 6) surrounded the fluoro benzene moiety in ritanserin after simulation 2 with ritanserin. The piperidine ring interacted with aromatic residues, $Trp^{326}$ and $Phe^{329}$ (transmembrane helix 6) after simulation 2 with ketanserin, and with $Phe^{329}$ after simulation 2 with ritanserin. These results are in agreement with results from ligand binding studies, which have suggested that the benzoyl portion of ketanserin-type compounds is important for high-affinity binding to 5-$HT_{2A}$ and 5-$HT_{2C}$ receptors (Herndon et al., 1992), and that the benzoyl carbonyl group in ketanserin-type compounds may have a prominent role in anchoring or orientating these compounds at the 5-$HT_{2A}$ receptor (Ismaiel et al., 1995). The present study suggests that ketanserin, an antagonist containing a benzoyl carbonyl group and ritanserin which do not contain such a group may differ in the manner in which they interact with the rat 5-$HT_{2C}$ receptor. Ligand binding studies have suggested multiple binding modes of ketanserin analogues at the rat 5-$HT_{2A}$ receptor, and that the benzoyl substituent is the most significant determinant of the manner in which these ligands bind to the 5-$HT_{2A}$ receptor (Ismaiel et al., 1995). These results do not support the hypothesis that structurally diverse antagonists interact in a similar orientation at the 5-$HT_{2A}$ receptor, as assumed in a pharmacophore model derived from series of 5-$HT_{2A}$ receptor antagonists (Andersen et al., 1994).

### 4.6. Receptor structure at the ligand binding site

The present simulations of the 5-$HT_{2C}$ receptor with ligands produced specific intramolecular hydrogen bonds in the cavity between the transmembrane helices, which may be essential for maintainance of the receptor structure and signal transduction (Table 6). $Asp^{100}$ was hydrogen-bonded to $Asn^{366}$ in transmembrane helix 7 after 4 out of 6 simulations of ligand–receptor complexes, and to $Asn^{72}$ in transmembrane helix 1 after all 6 simulations. These findings are in agreement with site-directed mutagenesis experiments with the human 5-$HT_{2A}$ receptor, which suggest that the hydrogen bond between $Asp^{120}$ in transmembrane helix 2 and $Asn^{376}$ in transmembrane helix 7 (corresponding to $Asp^{100}$ and $Asn^{366}$ in the rat 5-$HT_{2C}$ receptor) is important for signal transduction (Sealfon et al., 1995).

### 4.7. Structural changes induced by ligand binding

Based on the present calculations, we propose that ligand binding may lead to specific rearrangement of one

or more hydrogen bonds between the highly conserved residues in the central cavity of the 5-$HT_{2C}$ receptor. Some of the rearrangements (e.g. formation of the $Asp^{100}$–$Cys^{362}$ and $Tyr^{370}$–$Asn^{366}$ hydrogen bonds) that occurred during simulation 1 with serotonin, did not occur in any of the other simulations. A hydrogen bond between $Asp^{100}$ (transmembrane helix 2) and $Ser^{363}$ (transmembrane helix 7) was formed in all simulations except simulation 2 with ritanserin (Table 6). Such rearrangement of hydrogen bonds may affect interhelical interactions, which in turn may affect the conformation of intracellular loops that are involved in G-protein-coupling. Biological experiments have demonstrated that the binding of 13 different antagonists (often called 'inverse agonists'), including ketanserin, may lead to conformational changes in the intracellular loops of the rat 5-$HT_{2C}$ receptor, whereas binding of two other antagonists (+)2-bromolysergic acid diethylamide and methysergide (often called 'neutral antagonists') may lead to no such effects (Westphal and Sanders-Bush, 1994; Barker et al., 1994). By comparing models of ligand–receptor complexes for both these kinds of antagonists, it may be possible to identify differences in the manner which these compounds interact with the 5-$HT_{2C}$ receptor.

### 4.8. Comparision with ligand-5-$HT_{2A}$ receptor models

In a previous model of the rat 5-$HT_{2A}$ receptor, the transmembrane helices were packed in a circular arrangement (Edvardsen et al., 1992). Molecular dynamics simulations of receptor–ligand complexes, with serotonin, ritanserin (Edvardsen et al., 1992) and ketanserin (Kristiansen et al., 1993) positioned into this model, produced oval arrangements of the seven transmembrane helices, which did not closely resemble the helix arrangement suggested by (Baldwin, 1993), from the projection map of bovine rhodopsin (Schertler et al., 1993).

The seven transmembrane helices have been organized in an anticlockwise arrangement viewed from the synaptic side, in the order 1, 3, 4, 5, 6, 7, 2 in one rat 5-$HT_{2A}$ receptor model (Zhang and Weinstein, 1993) and in the order 1, 2, 3, 4, 5, 6, 7 in the majority of other rat 5-$HT_{2A}$ receptor models and in the present rat 5-$HT_{2C}$ receptor model. The transmembrane helices were packed according to the projection map of bovine rhodopsin (Schertler et al., 1993; Baldwin, 1993) both in the present model of the rat 5-$HT_{2C}$ receptor and in other recent models of G-protein-coupled receptors (Zhang and Weinstein, 1993; Zhou et al., 1994; Donnelly et al., 1994). In contrast to most other receptor models, the present model includes the loops between transmembrane helices, N- and C-terminals and a disulfide bridge between $Cys^{128}$ (transmembrane helix 3) and $Cys^{208}$ in the second extracellular loop.

Several different models of the serotonin–rat 5-$HT_{2A}$ receptor complex have been reported. The primary counterion for the protonated amine group in serotonin was the Asp in transmembrane helix 3, conserved among biogenic amine receptors, both in the present 5-$HT_{2C}$ receptor model ($Asp^{135}$ in transmembrane helix 3 of the rat 5-$HT_{2C}$ receptor) and in other rat 5-$HT_{2A}$ receptor models ($Asp^{155}$ in transmembrane helix 3 of the rat 5-$HT_{2A}$ receptor) (Zhang and Weinstein, 1993; Westkaemper and Glennon, 1993; Trumpp-Kallmeyer et al., 1992; Donnelly et al., 1994). This assumption is supported by results from site-directed mutagenesis experiments with the rat 5-$HT_{2A}$ receptor (Wang et al., 1993). The OH group of serotonin may be hydrogen-bonded to either $Ser^{239}$ in transmembrane helix 5 (Westkaemper and Glennon, 1993; Trumpp-Kallmeyer et al., 1992; Donnelly et al., 1994) or $Ser^{372}$ in transmembrane helix 7 (Zhang and Weinstein, 1993) (corresponding to $Ser^{220}$ and $Cys^{362}$ in the rat 5-$HT_{2C}$ receptor). All cloned serotonin receptors have either a Thr or a Ser residue in the position corresponding to $Ser^{220}$ (transmembrane helix 5) in the rat 5-$HT_{2C}$ receptor (Oliveira et al., 1993). Therefore, a hydrogen bond interaction between this residue and the OH group of serotonin seems likely. The indole NH group in serotonin may form a hydrogen bond with either $Ser^{159}$ in transmembrane helix 3 (Donnelly et al., 1994), $Ser^{203}$ (Trumpp-Kallmeyer et al., 1992), or $Ser^{207}$ in transmembrane helix 4 (Westkaemper and Glennon, 1993) in the rat 5-$HT_{2A}$ receptor (corresponding to $Ser^{139}$, $Ser^{183}$ and $Ser^{187}$ in the rat 5-$HT_{2C}$ receptor). $Ser^{139}$ and $Ser^{183}$ are conserved among all 5-$HT_2$ receptor subtypes, whereas $Ser^{187}$ not is conserved among 5-$HT_2$ receptor subtypes (Ser in the 5-$HT_{2A}$ and 5-$HT_{2C}$ receptors, Ala in the 5-$HT_{2B}$ receptor) (Oliveira et al., 1993). After simulation 1 with serotonin, $Ser^{133}$ in transmembrane helix 3 and the main-chain carbonyl groups of $Val^{186}$ in transmembrane helix 4 and $Ala^{223}$ in transmembrane helix 5 in the rat 5-$HT_{2C}$ receptor were hydrogen-bonded to the polar indol groups in serotonin. As observed in the present rat 5-$HT_{2C}$ receptor model, $Phe^{243}$ in transmembrane helix 5 and $Phe^{340}$ in transmembrane helix 6, in the rat 5-$HT_{2A}$ receptor (corresponding to $Phe^{224}$, $Phe^{330}$ in the rat 5-$HT_{2C}$ receptor) have been proposed to interact with the indole ring in serotonin (Trumpp-Kallmeyer et al., 1992; Westkaemper and Glennon, 1993; Donnelly et al., 1994).

A previous model of the 5-$HT_{2A}$ receptor with ritanserin showed preference for a ligand orientation, with the fluoro benzene moiety oriented towards the synaptic side (Edvardsen et al., 1992), which was different from the present ritanserin-5-$HT_{2C}$ receptor model. In the present model, the protonated piperdine NH group of ritanserin was oriented towards the side-chain carboxyl group of $Asp^{135}$. The majority of residues interacting with ritanserin were in transmembrane helices 3, 4, 6, 7. In spite of the fact that ritanserin was differently orientated in the present 5-$HT_{2C}$ receptor model and in the previous 5-$HT_{2A}$ receptor model, several residues interacted strongly with the antagonist in both models, e.g. $Asp^{135}$ in transmembrane helix 3, $Trp^{180}$ in transmembrane helix 4 and $Trp^{326}$, $Phe^{329}$ and $Asn^{333}$ in transmembrane helix 6 (rat 5-$HT_{2C}$

receptor). However, $Cys^{362}$ and $Ser^{363}$ in transmembrane helix 7 also interacted particularly strongly with ritanserin in the present 5-$HT_{2C}$ receptor model, whereas interactions with the corresponding residues were not observed in the previous model of the ritanserin–5-$HT_{2A}$ receptor complex. $Asp^{120}$ and $Met^{128}$ in transmembrane helix 2 interacted particularly strongly with ritanserin in our previous 5-$HT_{2A}$ receptor model, whereas interactions with the corresponding $Asp^{100}$ and $Met^{108}$ residues were weak or absent in the present model of the ritanserin–5-$HT_{2C}$ receptor complex. $Trp^{336}$ and $Phe^{339}$ (transmembrane helix 6) were involved in aromatic–aromatic interactions with the fused ring system in ritanserin in our previous model, and in aromatic–aromatic interactions with the fluoro benzene rings in ritanserin in the present model.

An orientation of ketanserin at the putative binding site of the rat 5-$HT_{2A}$ receptor model which was similar to that proposed in the present study, produced the lowest ketanserin–receptor interaction energy (Kristiansen et al., 1993). The majority of residues interacting with ketanserin were in transmembrane helices 3–7 in the present model. Ketanserin interacted particularly strongly with $Ala^{223}$ in transmembrane helix 5, $Phe^{322}$, $Asn^{333}$ in transmembrane helix 6 and $Ile^{358}$ in transmembrane helix 7 in the present model, whereas interactions with the corresponding residues were weak or absent in the previous model of the ketanserin–5-$HT_{2A}$ receptor complex. Ketanserin interacted particularly strongly with $Asp^{120}$ in transmembrane helix 2, $Trp^{151}$ in transmembrane helix 3, $Phe^{240}$, $Phe^{243}$ in transmembrane helix 5 in the previous 5-$HT_{2A}$ receptor model (corresponding to $Asp^{100}$, $Trp^{131}$, $Phe^{221}$, $Phe^{224}$ in the rat 5-$HT_{2C}$ receptor), whereas interactions with the corresponding residues were weak or absent in the present model of the ritanserin–5-$HT_{2C}$ receptor complex. In our previous 5-$HT_{2A}$ receptor model, the phenyl ring of $Phe^{243}$ was stacked with the fluoro benzene ring in ketanserin, whereas the corresponding $Phe^{224}$ interacted with the quinazolindione ring in the present model.

Although models of G-protein-coupled receptors should be regarded as approximate three-dimensional structures, and conflicting structures have been proposed for the same receptors, these constructs have proven to be useful in structure–functional analysis of G-protein-coupled receptors (Luo et al., 1994).

## 5. Conclusions

Strongest antagonist–receptor interactions were obtained after simulations with the *p*-fluoro benzene moiety of ketanserin and ritanserin oriented towards the cytoplasmic side of the receptor model. Slightly different orientations and receptor interactions of ketanserin and ritanserin were predicted. The following residues were proposed to be involved in aromatic–aromatic interactions with the fluoro benzene ring(s) in the antagonists: $Phe^{138}$ (transmembrane helix 3), $Trp^{180}$ (transmembrane helix 4), $Phe^{322}$, $Trp^{326}$ (transmembrane helix 6), $Phe^{329}$ (transmembrane helix 6). The present antagonist–receptor complexes suggest that $Asn^{333}$ (transmembrane helix 6) may form a hydrogen-bonding interaction and $Ala^{223}$ (transmembrane helix 5) a strong van der Waals interaction with the fused ring system in ketanserin, but not in ritanserin. The indole ring in serotonin may interact with $Phe^{224}$, $Pro^{227}$ in transmembrane helix 5, $Trp^{326}$ and $Phe^{330}$ in transmembrane helix 6. $Asp^{100}$ in transmembrane helix 2 may form hydrogen bonds with $Asn^{72}$, $Asn^{366}$ and $Tyr^{370}$ in the 5-$HT_{2C}$ receptor. These hypotheses may be tested by site-directed mutagenesis and ligand binding experiments, which would lead to a more accurate receptor model, which may be used for structure based design of specific 5-$HT_{2C}$ receptor ligands.

### *Supplementary material available*

The AMBER parameters, atomic charges for serotonin, ketanserin and ritanserin and atomic coordinates for energy-minimized ligand–receptor complexes after simulations are available from the authors upon request.

## Acknowledgements

Supported by grants from the Research Council of Norway, Norsk Medisinaldepot and from the Norwegian Supercomputing Committee.

## References

Andersen, K., T. Liljefors, K. Gundertofte, J. Perregaard and K.P. Bøgesø, 1994, Development of a receptor–interaction model for serotonin 5-$HT_2$ receptor antagonist. Prediction selectivity with respect to dopamine $D_2$ receptors, J. Med. Chem. 37, 950.

Baldwin, J.M., 1993, The probable arrangement of the helices in G protein-coupled receptors, EMBO J. 12, 1693.

Baldwin, J.M., 1994, Structure and function of receptors coupled to G proteins, Curr. Opin. Cell. Biol. 6, 180.

Ballesteros, J.A. and H. Weinstein, 1994, Integrated methods for the construction of three dimensional models and computational probing of structure–function relations in G-protein coupled receptors, Methods Neurosci. 25, 366.

Barker, E.L., R.S. Westphal, D. Schmidt and E. Sanders-Bush, 1994, Constitutive active 5-hydroxytryptamine$_{2C}$ reveal novel inverse agonist activity of receptor ligands, J. Biol. Chem. 269, 11687.

Boess, F.G. and I.L. Martin, 1994, Molecular biology of 5-HT receptors, Neuropharmacology 33, 275.

Choudhary, M.S., S. Craigo and B.L. Roth, 1992, Identification of receptor domains that modify ligand binding to 5-hydroxytryptamine$_2$ and 5-hydroxytryptamine$_{1c}$ serotonin receptors, Mol. Pharmacol. 42, 627.

Choudhary, M.S., S. Craigo and B.L. Roth, 1993, A single point mutation ($Phe^{340} \rightarrow Leu^{340}$) of a conserved phenylalanine abolishes 4-[$^{125}$]Iodo-(2,5-dimethoxy)phenylisopropylamine and [$^3$H]-mesulergine

but not [$^3$H]-ketanserin binding to 5-hydroxytryptamine$_2$ receptors, Mol. Pharmacol. 43, 755.

Choudhary, M.S., N. Sachs, A. Uluer, R.A. Glennon, R.B. Westkaemper and B.L. Roth, 1995, Differential ergoline and ergopeptine binding to 5-hydroxytryptamine$_{2A}$ receptors: ergolines require an aromatic residue at position 340 for high affinity binding, Mol. Pharmacol. 47, 450.

Dahl, S.G., Ø. Edvardsen and I. Sylte, 1991, Molecular dynamics of dopamine at the $D_2$ receptor, Proc. Natl. Acad. Sci. USA 88, 8111.

Deisenhofer, J. and H. Michel, 1989, The photosynthetic reaction center from the purple bacterium Rhodopseudomonas viridis, Science 245, 1463.

Donnelly, D., J.B.C. Findlay and T.L. Blundell, 1994, The evolution and structure of aminergic G protein-coupled receptors, Receptors Channels 2, 61.

Dudley, M., A. Ogden, A. Carr, T. Nieduzak and J. Kehne, 1990, MDL 100,907, (+)-α-(2,3-dimethoxyphenyl)-1-[2-(4-fluorophenylethyl)-4-piperidine methanol, a potent, chiral, 5-HT$_2$ receptor antagonist, Soc. Neurosci. Abstr. 16, 1037.

Edvardsen, Ø., I. Sylte and S.G. Dahl, 1992, Molecular dynamics of serotonin and ritanserin interacting with the 5-HT$_2$ receptor, Mol. Brain. Res. 14, 166.

Ferrin, T.E., C.C. Huang, L.E. Jarvis and R. Langridge, 1988, The MIDAS display system, J. Mol. Graphics 6, 13.

Forbes, I.T., G.A. Kennett, A. Gadre, P. Ham, C.J. Hayward, R.T. Martin, M. Thomson, M.D. Wood, G.S. Baxter, A. Glen, O.E. Murphy, B.A. Stewart and T.P. Blackburn, 1993, *N*-(1-methyl-5-indolyl)-*N'*-(3-pyridyl)urea hydrochloride: the first selective 5-HT$_{1C}$ receptor antagonists, J. Med. Chem. 36, 1104.

Garnier, J., D.J. Osguthorpe and B. Robson, 1978, Analysis of the accuracy and implications of simple methods for prediction the secondary structure of globular proteins, J. Mol. Biol. 120, 97.

Glennon, R.A., R.B. Westkaemper and P. Bartyzel, 1991, The medicinal chemistry of serotonergic agents, in: Serotonin Receptor Subtypes. Basic and Clinical Aspects, ed. S.J. Peroutka (Wiley-Liss, New York) p. 19.

Glennon, R.A., M. Dukat, M. El-Bermawy, H. Law, J. De Los Angeles, M. Teitler, A. King and K. Herrick-Davis, 1994, Influence of amine substituents on 5-HT2A versus 5-HT2C binding of phenylalkyl- and indolylalkylamines, J. Med. Chem. 37, 1929.

Henderson, R., J.M. Baldwin, T.A. Ceska, F. Zemlin, E. Beckman and K.H. Downing, 1990, Model for the structure of bacteriorhodopsin based on high resolution electron cryo-microscopy, J. Biol. Chem. 213, 899.

Herndon, J.L., A. Ismaiel, S.P. Ingher, M. Teitler and R.A. Glennon, 1992, Ketanserin analogues: structure–affinity relationships for 5-HT$_2$ and 5-HT$_{1c}$ serotonin receptor binding, J. Med. Chem. 35, 4903.

Humphrey, P.P.A., P. Hartig and D. Hoyer, 1993, A proposed new nomenclature for 5-HT receptors, Trends Pharmacol. Sci. 14, 233.

Ismaiel, A.M., K. Arruda, M. Teitler and R.A. Glennon, 1995, Ketanserin analogues: the effect of structural modification on 5-HT2 serotonin receptor binding, J. Med. Chem. 38, 1196.

Julius, D., K.N. Huang, T.J. Livelli, R. Axel and T.M. Jessell, 1990, The 5-HT$_2$ receptor defines a family of structurally distinct but functionally conserved serotonin receptors, Proc. Natl. Acad. Sci. USA 87, 928.

Kolakowski, L.F.J., 1994, GCRDb: a G protein-coupled receptor database, Receptors Channels 2, 1.

Kristiansen, K., Ø. Edvardsen and S.G. Dahl, 1993, Molecular modeling of ketanserin and its interactions with the 5-HT$_2$ receptor, Med. Chem. Res. 3, 370.

Leonhardt, S., K. Herrick-Davis, B.D. Wilcox and B.J. Hoffman, 1993, Site-specific mutagenesis demonstrated that arginine 195 in TMD 4 is a critical determinant for agonist affinities at the 5-HT$_{1c}$ and 5-HT$_2$ receptors, Soc. Neurosci. Abstr. 19, 1165.

Luo, X., D. Zhang and H. Weinstein, 1994, Ligand-induced domain motion in the activation mechanism of a G-protein-coupled receptor, Protein Eng. 7, 1441.

Nelson, D.L., 1993, The serotonin$_2$ (5-HT$_2$) subfamily of receptors: pharmacological challenges, Med. Chem. Res. 3, 306.

Oliveira, L., A.C.M. Paiva and G. Vriend, 1993, A common motif in G-protein-coupled seven transmembrane helix receptors, J. Comput. Aided Mol. Design 7, 649.

Pardo, L., J.A. Ballesteros, R. Osman and H. Weinstein, 1992, On the use of the transmembrane domain of bacteriorhodopsin as a template for modelling the three-dimensional structure of guanine nucleotide-binding regulatory protein-coupled receptors, Proc. Natl. Acad. Sci. USA 89, 4009.

Pearlman, D.A., D.A. Case, J.C. Caldwell, G.L. Seibel, U.C. Singh, P. Weiner and P.A. Kollman, 1991, AMBER 4.0 (University of California, San Francisco)

Peroutka, S.J., 1994, Molecular biology of serotonin (5-HT) receptors, Synapse 18, 241.

Pierce, P.A., J.Y. Kim and S.J. Peroutka, 1992, Molecular structural basis of ligand selectivity for 5-HT$_2$ versus 5-HT$_{1C}$ cortical receptors, Naunyn Schmiedebergs Arch. Pharmacol. 346, 4.

Schertler, G.F.X., C. Villa and R. Henderson, 1993, Projection structure of rhodopsin, Nature 362, 770.

Schmuck, K., C. Ullmer, P. Engels and H. Lübbert, 1994, Cloning and functional characterization of the human 5-HT$_{2B}$ serotonin receptor, FEBS Lett. 342, 85.

Sealfon, S.C., L. Chi, B.J. Ebersole, V. Rodic, D. Zhang, J.A. Ballesteros and H. Weinstein, 1995, Related contribution of specific helix 2 and 7 residues to conformational activation of the serotonin 5-HT$_{2A}$ receptor, J. Biol. Chem. 270, 16683.

Trumpp-Kallmeyer, S., J. Hoflack, A. Bruinvels and M.F. Hibert, 1992, Modeling of G-protein-coupling receptors: application to dopamine, adrenaline, serotonin, acetylcholine, and mammalian opsin receptor, J. Med. Chem. 35, 3448.

Van Wijngaarden, I., M.T.M. Tulp and W. Soudijn, 1990, The concept of selectivity in 5-HT receptor research, Eur. J. Pharmacol. Mol. Pharmacol. 188, 301.

Wang, C.-D., T.K. Gallaher and J.C. Shih, 1993, Site-directed mutagenesis of the serotonin 5-hydroxytryptamine$_2$ receptor: identification of amino acids necessary for ligand binding and receptor activation, Mol. Pharmacol. 43, 931.

Wang, H.Y., L. Lipfert, C.C. Malbon and S. Bahout, 1989, Site-directed anti-peptide antibodies define the topography of the β-adrenergic receptor, J. Biol. Chem. 264, 14424.

Weiner, S.J., P.A. Kollman, D.A. Case, U.C. Singh, C. Ghio, G. Alagona, S. Profeta Jr. and P. Weiner, 1984, A new force field for molecular mechanical simulation of nucleic acids and proteins, J. Am. Chem. Soc. 106, 765.

Wess, J., S. Nanavati, Z. Vogel and R. Maggio, 1993, Functional role of proline and tryptophan residues highly conserved among G protein-coupled receptors studied by mutational analysis of the m3 muscarinic receptor, EMBO J. 12, 331.

Westkaemper, R.B. and R.A. Glennon, 1993, Molecular graphics models of members of the 5-HT2 subfamily: 5-HT$_{2A}$, 5-HT$_{2B}$ and 5-HT$_{2C}$ receptors, Med. Chem. Res. 3, 317.

Westphal, R.S. and E. Sanders-Bush, 1994, Reciprocal binding properties of 5-hydroxytryptamine type 2C receptor agonists and inverse agonists, Mol. Pharmacol. 46, 937.

Zhang, D. and H. Weinstein, 1993, Signal transduction by a 5-HT$_2$ receptor: a mechanistic hypothesis from molecular dynamics simulations of the three-dimensional model of the receptor complexed to ligands, J. Med. Chem. 36, 934.

Zhou, W., C. Flanagan, J.A. Ballesteros, K. Konvicka, J.S. Davidson, H. Weinstein, R.P. Millar and S.C. Sealfon, 1994, A reciprocal mutation supports helix 2 and helix 7 proximity in the gonadotropin-releasing hormone receptor, Mol. Pharmacol. 45, 165.